Formation of Mangala Fossa, the source of the Mangala Valles, Mars: Morphological development as a result of volcano-cryosphere interactions

Harald J. Leask,[1] Lionel Wilson,[1] and Karl L. Mitchell[1,2]

[1]   The morphology of the Mangala Fossa graben forming the source of the Mangala Valles implies that two episodes of graben subsidence took place, each induced by lateral dike intrusion from Arsia Mons. Quantitative modeling suggests that graben boundary faults breaching the cryosphere provided pathways for water release from an underlying aquifer at a peak rate of $\sim 10^7$ m^3 s^{-1}. In the first event, the graben subsided by $\sim$200 m, and water carrying a thin ice layer filled the graben, overflowing after $\sim$2.5 hours, mainly at a low point on the north rim. This captured the water flux, eroding a gap in the north wall which, with an erosion rate of $\sim$100 μm s^{-1} and a duration of $\sim$1 month, was $\sim$250 m deep by the end of water release. Erosion of the graben floor also took place, at $\sim$20 μm s^{-1}, lowering it by $\sim$50 m. Subsequently, heat from the cooling dike melted cryosphere ice, causing a further $\sim$150 m of subsidence on compaction. In the second event, with a similar duration and peak discharge, the graben again subsided by $\sim$200 m and filled with ice-covered water until overflow through the gap began at a water depth of $\sim$350 m. The gap was eroded down by a further $\sim$400 m, and the floor was eroded by a further $\sim$50 m. Finally, heat from the second dike sublimed cryosphere ice, lowering the floor by $\sim$100 m. In places, combined erosion and subsidence of the graben floor exposed $\sim$200 m of the first dike.

1.   Introduction

[2]   A series of graben systems, the Memnonia, Sirenum, Icaria, Thaumasia, and Claritas fossae (Figures 1 and 2) are present in the region to the southwest, south, and southeast of Arsia Mons, one of the three large shield volcanoes located on the Tharsis rise, the most extensive volcanic province on Mars [e.g., *Zimbelman et al.*, 1992; *Cattermole*, 2001]. The Memnonia Fossae are the most northerly of these graben, and one of them, labeled Mangala Fossa [*U.S. Geological Survey*, 2003] in Figure 1, is the source for the Mangala Valles (Figure 3), a major outflow channel system [*Sharp and Malin*, 1975; *Malin*, 1976; *Nummedal et al.*, 1976; *Carr and Clow*, 1981; *Tanaka and Chapman*, 1990; *Zimbelman et al.*, 1992; *Head and Wilson*, 2001; *Ghatan et al.*, 2004, 2005; *Head et al.*, 2004; *Wilson and Head*, 2004; *Wilson et al.*, 2004a, 2004b; *Hanna and Phillips*, 2005a; *Leask*, 2005] (also *Craddock and Greeley* [1994], as cited by *Plescia* [2003]). The channel system is probably of Late Hesperian to Early Amazonian age [e.g., *Tanaka and Chapman*, 1990], and can

be traced to a $\sim$650 m deep gap that breaches the north rim of the graben at about 18.4°S, 210.5°E, and connects the interior of the graben to a broad valley leading toward the lowlands of Amazonis Planitia further to the north. We concur with most previous authors in inferring that the great length and general morphology of the channel system preclude formation by fluids other than water [e.g., *Hoffman*, 2000], and that the only logical interpretation of the morphology of Mangala Fossa is that the graben filled with water which then overflowed, eroding the gap [*Zimbelman et al.*, 1992; *Head and Wilson*, 2001; *Ghatan et al.*, 2004; *Head et al.*, 2004; *Wilson and Head*, 2004; *Leask*, 2005]. There is evidence that two water release events may have been needed to form the Mangala Valles system in its present form [*Chapman and Tanaka*, 1990; *Tanaka and Chapman*, 1990; *Zimbelman et al.*, 1992; *Fuller and Head*, 2002a, 2002b; *Ghatan et al.*, 2004, 2005], and so the morphology of the graben in general, and particularly the gap in its north wall, may likewise represent the accumulated effects of two water flow events [*Leask*, 2005].

[3]   We explicitly assume that the source of the water was an aquifer system trapped beneath the impervious cryosphere, the outer few kilometers of the crust where the temperature is less than the freezing point of water and pore space is occupied by ice [*Clifford*, 1987, 1993; *Carr*, 1996]. *Wilson and Head* [2002] suggested that the Memnonia Fossae and other fossae in this region were produced by the intrusion of dikes propagating laterally from Arsia Mons

[1]Planetary Science Research Group, Environmental Science Department, Institute of Environmental and Natural Sciences, Lancaster University, Lancaster, UK.
[2]Jet Propulsion Laboratory, Pasadena, California, USA.
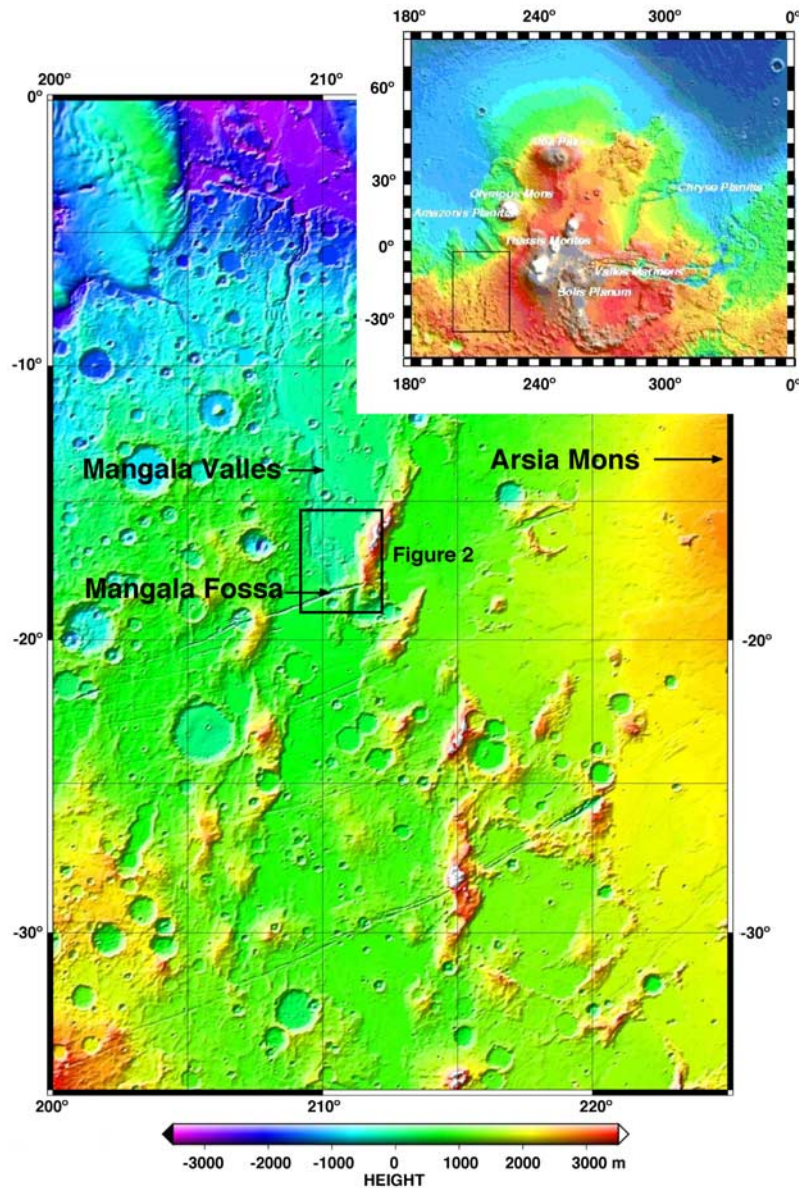
Figure 1.   Color-coded MOLA topography of Mangala Valles floodplain, Mangala Fossa source graben, and highland topography containing proposed aquifer system feeding the valley. Box shows location of Figure 2. Inset is of Tharsis volcanic area.

(Figure 1). The dike tops were trapped at shallow depth underneath the surface by the combination of stresses due to the excess pressure in the magma (acting to widen the dike) and regional loading and tectonic stresses (acting to close it) [*Mastin and Pollard*, 1988; *Rubin*, 1992; *Head and Wilson*, 2001; *Wilson and Head*, 2001]. Topographic evidence that some Martian graben are produced by dikes is growing [*Schultz et al.*, 2004], and specific evidence for the presence of at least one dike beneath the eastern part of Mangala Fossa is provided by the presence of what are interpreted by *Wilson and Head* [2004] to be the deposits of a phreato-magmatic eruption. The induced graben boundary faults, together with the underlying dike itself, would have pro-vided a system of fractures penetrating the cryosphere and facilitating water release. In this paper we assume that water reached the surface along one or both of the graben faults. Soon after the first flood event ended, residual water in the

parts of the fracture systems within the cryosphere would have frozen. To allow the initiation of the second flood event, either a new set of fractures must have formed or the old fractures must have been reactivated. We take this to imply that a second volcanic intrusion occurred to cause the second flood. The fact that phreatomagmatic volcanic activity took place attests to the presence of ice and/or water at shallow depths at the time of at least one of the dike intrusions, and further evidence comes from the morphology of the impact crater located just south of Mangala Fossa at 18.9°S, 210.5°E. Lobate, ''muddy'' ejected material is present around the crater on both the north and south sides of the graben, but there appears to be no ejecta present on the graben floor (see Figure 3). The nature of the ejecta strongly suggests that a cryosphere existed in this area at the time of crater formation [*Carr et al.*, 1977; *Tanaka and Chapman*, 1990; *Squyres et al.*, 1992], and the absence of
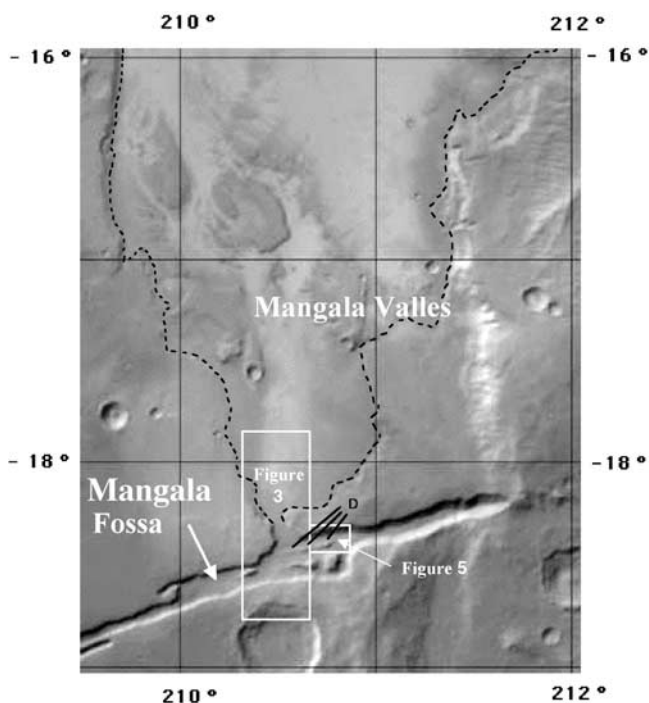
Figure 2. Low-resolution MOC mosaic of Mangala Valles and Mangala Fossa showing outflow channel (maximum extent indicated by dashed line) radiating from ~5 km wide breach in north wall of graben. Proposed dike outcrops are indicated (D). Boxes show locations of Figures 3 and 5. Each degree is ~60 km.

ejecta on the graben floor implies that the second flood event must have occurred after the impact crater was formed [*Tanaka and Chapman*, 1990; *Leask*, 2005].

[4] Water release triggered by interactions between volcanic intrusions and the cryosphere has occurred in many places on Mars [e.g., *Carr*, 1979, 1987; *Tanaka and Chapman*, 1990; *Baker et al.*, 1991; *Tanaka et al.*, 1991]. Water release due to dike intrusion, as occurred at Mangala Fossa, is inferred to have happened in Elysium, where the Athabasca Valles channel system is sourced from one of the Cerberus Fossae graben [*Burr et al.*, 2002a, 2002b; *McEwen et al.*, 2002; *Manga*, 2004; *Mitchell et al.*, 2005]. The Athabasca and the Mangala source areas each have distinctive characteristics. At Athabasca the width of the source graben in the water release zone is similar to that elsewhere along its length, and there is evidence in the form of surface erosion for a few kilometers on either side of the graben that a large water fountain formed due to the high speed of the water rising through the cryosphere fracture [*Head et al.*, 2003]. The implication is that water escaped from the graben mainly through the fountain, rather than simply filling the graben and overflowing. There is no indication in the immediate vicinity of the water source of eruption of magma from the underlying dike (though eruptions did occur elsewhere along the graben [*Berman and Hartmann*, 2002; *McEwen et al.*, 2002]). At Mangala, in contrast, the dike forming the Mangala Fossa graben penetrated far enough into the cryosphere along part of its length near the eastern end to cause a phreatomagmatic eruption [see *Wilson and Head*, 2004]. There is no indica-
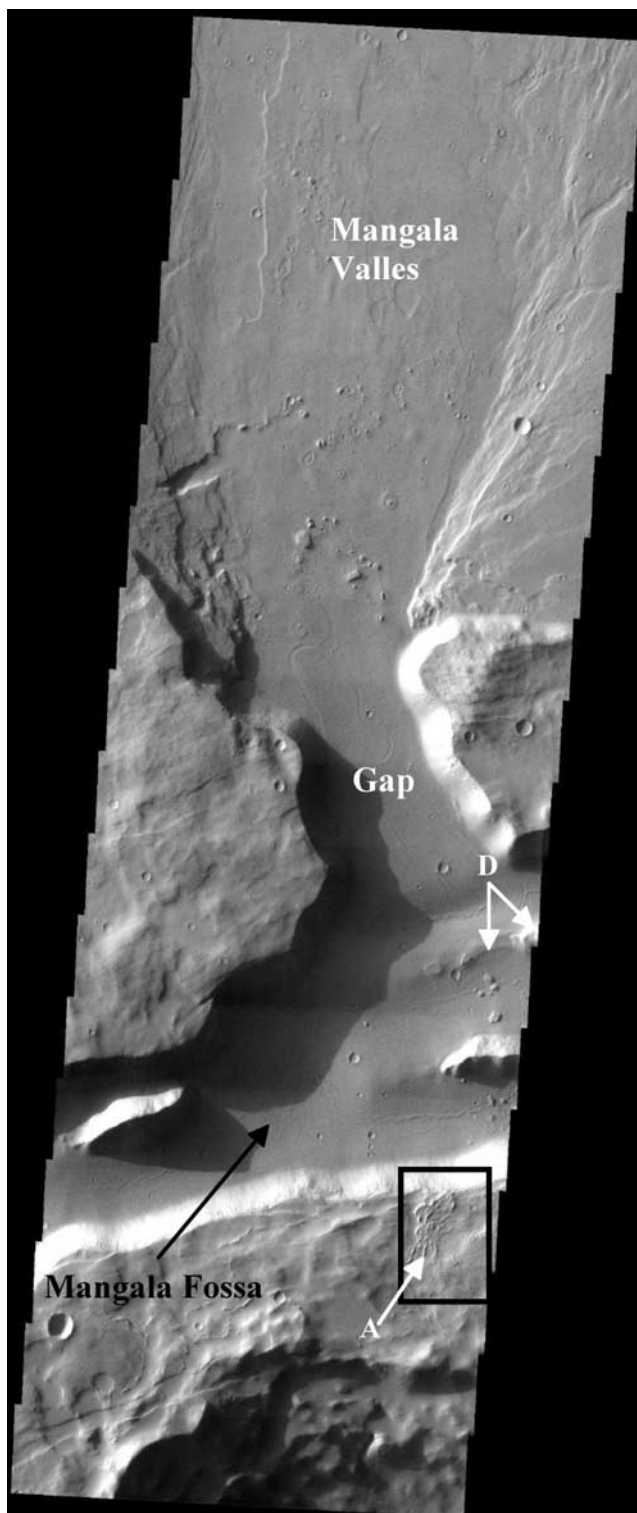
Figure 3. THEMIS-VIS image of Mangala Valles, showing an area of material (A), next to the south rim of Mangala Fossa, different in texture from the surrounding terrain. This may have been caused by overflowing water which turned to ice. Outcrop of dike (D) is indicated. North is to the top of THEMIS image V04762003.
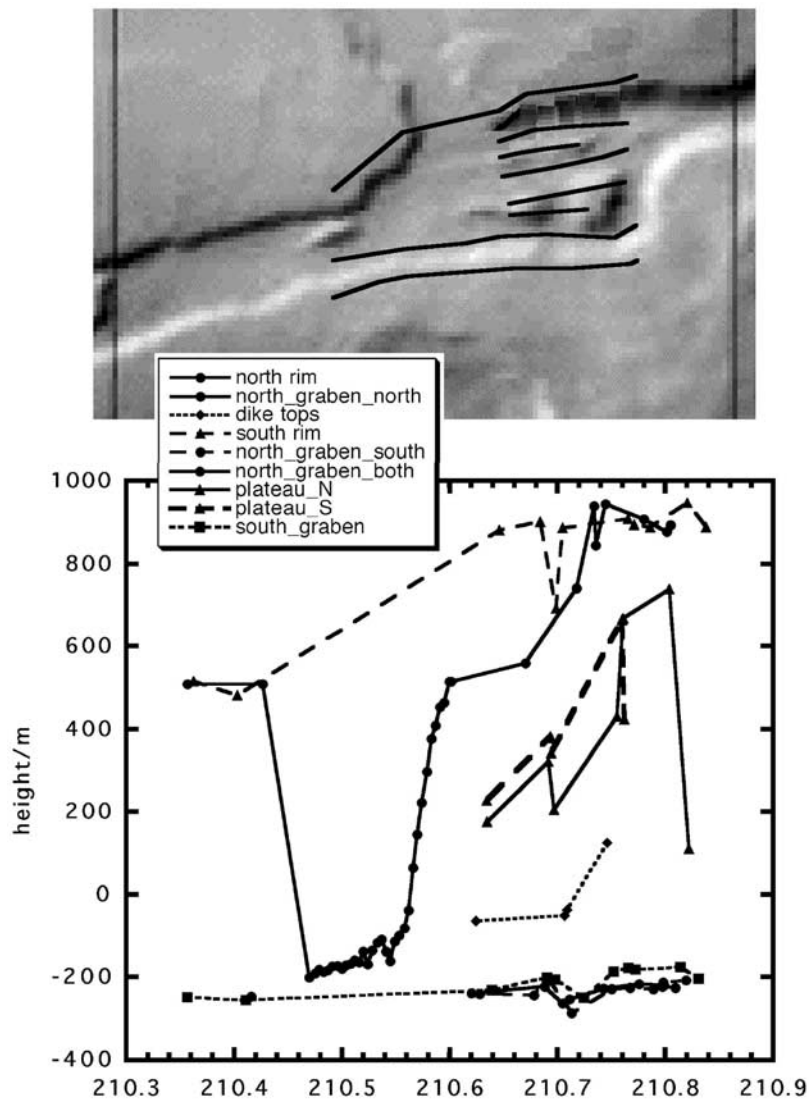
Figure 4. Topographical profiles, parallel to the strike of the Mangala Fossa graben, of the north and south rims of the graben, the gap in the north wall, the north and south plateaus, the tops of the proposed dikes, and parts of the graben floor. Elevations were extracted from all available MOLA profiles; see text for details. Image shows locations of profiles. Vertical lines indicate longitudes 210 and 211°E. At this latitude, each degree of longitude represents ∼56 km.

tion of a water fountain overtopping the graben rim; rather, the outflow of water through the gap implies that the graben filled and overflowed in a less violent manner.

[5] In this paper we use altimetry from the Mars Orbiter Laser Altimeter (MOLA) on Mars Global Surveyor (MGS), together with images from the Mars Orbiter Camera (MOC) on MGS and the Thermal Emission Imaging Spectrometer (THEMIS) on Mars Odyssey, to define the detailed morphology of Mangala Fossa. We attempt to relate this to a proposed sequence of events that took place while two dike intrusions and associated flood events were in progress.

2. Morphology of Mangala Fossa

[6] Mangala Fossa has a continuously connected length of ∼210 km (Figure 1). With the exception of the region near the gap connecting it with the Mangala Valles, its width is typically ∼2 km, similar to the 1–2 km mean width of

other members of the Memnonia Fossae graben group [*Wilson and Head*, 2002], and near its eastern end, where a phreatomagmatic eruption took place [*Wilson and Head*, 2004], its width averages ∼4.7 km (Figure 2). In the vicinity of the gap the structure is more complex, with the northern and southern en echelon segments being essentially in contact (Figure 2). The width of the northern segment here is ∼4.5 km with a total width across the two of ∼9.9 km.

[7] Figure 4 shows how the absolute levels (relative to the Mars MOLA datum) of the north and south rims of Mangala Fossa vary along strike (approximately WSW–ENE) in the vicinity of the gap breaching the north wall of the graben. Elevations were extracted from all standard MOLA profiles that cross the area by taking data points as close as possible to the rim. It is clear that the south rim is generally higher than the north rim, and that the gap is located at the lowest point on the north rim. Thus the inference by all previous workers that the gap was eroded by water spilling over the
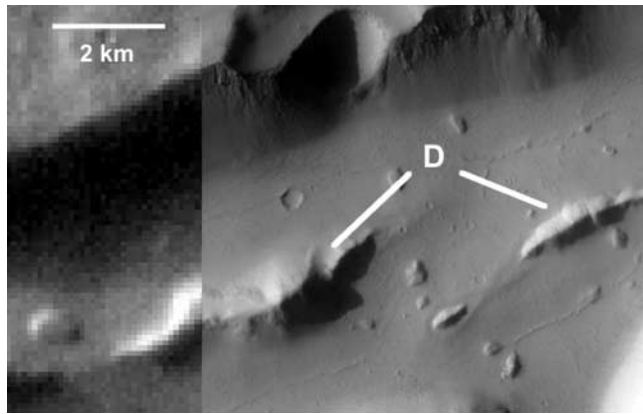
Figure 5. Mosaic of parts of THEMIS images (left) I04762002 and (right) V10329003 showing the highest proposed dike outcrops (D) on the floor of the Mangala Fossa, near the source of the Mangala Valles. North is to the top.

lowest point on the rim when the graben became filled with water seems entirely justified. There is other evidence that the graben was filled with water at some time. In a few places, patches of ridged ground are present on the highland terrain immediately adjacent to the rim. One, located near the gap, is shown at "A" in Figure 3, and *Head et al.* [2004] show similar patches on both sides of the graben near the graben's eastern end. The texture of the surface in these areas led *Head et al.* [2004] to suggest that they are the results of sheets of ice having been present. We infer that this ice formed a thin layer on the surface of the lake of water rising in the graben as it filled. Water initially overflowed the rim of the graben in a few relatively low-lying places in addition to the location that was soon eroded to form the gap [*Head et al.*, 2004]. In these other places ice was rafted over the surrounding ground on a thin water layer. As soon as the gap had eroded downward (and possibly sideways) to reach a cross-sectional area capable of carrying the water flux entering the graben from below, water overflow in these other locations ceased. The ice rafts quickly became frozen to the local surface, and may then have deformed slowly under gravity, while simultaneously subliming into the atmosphere, to produce the surface deposits and textures seen today. We attempt to quantify these processes in section 6.

[8] In the region to the east of the gap, Figure 4 shows that the depth of the graben below its rim varies from 800 to 1100 m with a mean of about 900 m [*Leask*, 2005]. In the immediate vicinity of the gap and to the west, the depth is ∼750 m. In terms of its depth the graben is thus significantly different from the other members of the Memnonia Fossae graben group, which have depths of typically 100–200 m, ranging up to 450 m [*Wilson and Head*, 2002]. If, as we infer, the present graben is the result of two dike intrusion events, we might expect its depth to be double the values for the other similar graben, that is, 200–400 m, with a possible maximum of 900 m, which is consistent with the depths currently observed. However, we do not think that the present depth of the graben can be entirely due to floor subsidence along boundary faults as a result of the two dike intrusions, for reasons discussed in section 3.

[9] Figure 4 includes the east–west profile of the gap breaching the north wall of the graben. Unfortunately, no MOLA profiles cross the gap, and so we were forced to rely on a photoclinometric (shape from shading) method applied to MOC images to deduce the local topography in the form of a series of approximately east–west profiles locked to MOLA elevations on either side of the gap. This leads to a few tens of meters uncertainty in absolute elevations within the gap [*Leask*, 2005], but it is clear that in the vicinity of the gap the present floor of the graben is ∼100 m below the level of the floor of the gap.

[10] A number of low, approximately aligned, elongate ridges are present on the floor of the northern branch of the Mangala Fossa graben (Figure 5). The location of these ridges near the centerline of the northernmost graben segment, and their alignment with the local strike of that segment, leads to the hypothesis that these may be outcrops of the top of the first dike segment, the one involved in the formation of this part of the graben, rather than small residual horsts. In cross section these ridges appear triangular, implying that they are heavily eroded. If the average width of the three lowest ridges, ∼540 m, is reconstructed to vertical, it suggests that the original dike thickness was ∼270 m. This value fits well within the range (up to 600 to 700 m) predicted by *Wilson and Head* [2002] for giant dikes on Mars. The tops of the ridges lie at depths of ∼600 to 800 m below the adjacent north wall of the graben, so that they extend 200 to 300 m above the current graben floor (Figure 4). The greatest elevation of these ridges, i.e., the greatest proximity of the inferred dike tops to the preexisting surface, occurs at the eastern end of the group, perhaps consistent with the fact that this is the location of the phreatomagmatic eruption deposit described by *Wilson and Head* [2004].

3. Interpretation of Morphology

[11] We base our interpretation of the events that have shaped Mangala Fossa on three key observations. First, the present depth (∼750 m) and width (∼4 km) of the graben in the vicinity of the gap in the north wall are both more than double the values measured for other graben in the region. Second, the ∼100 m difference in height between the present graben floor and the floor of the gap, together with the colinearity of the graben floor-step contact and the northern graben boundary fault, can only reasonably be ascribed to the subsidence of the graben floor after the second flood event ceased. Presumably this was due to desiccation and compaction of the cryosphere by heat from the second dike. Third, if, as we infer, the elongate structures on the graben floor, which are at least 200 m high, are outcrops of the first dike, then the floor of the graben produced by that first intrusion must have suffered significant additional erosion by flowing water and/or subsidence by cryosphere compaction; this could have occurred after the first intrusion, after the second intrusion, or after each of the two events.

[12] How large might these various contributors to floor lowering have been? The overall average of a large number of depth measurements on other graben in the region is ∼200 m [*Wilson and Head*, 2002], and we adopt this as our nominal estimate of the graben subsidence resulting from each of the two intrusion events at Mangala Fossa. We infer
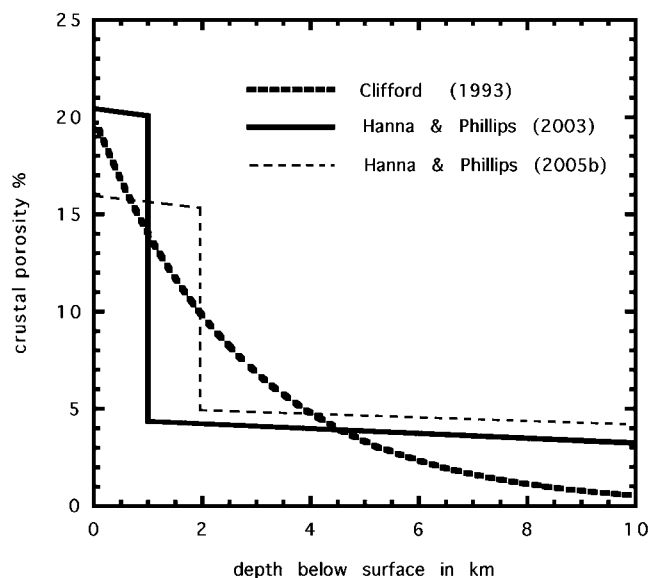
Figure 6. Porosity of outer 10 km of Martian cryosphere based on models of *Clifford* [1993] and *Hanna and Phillips* [2003, 2005b].

the amount of cryosphere subsidence that took place after each intrusion as follows. Plausible values for the geothermal gradient and mean surface temperature on Mars at the time of the Mangala Fossa activity (Late Hesperian to Early Amazonian [*Tanaka and Chapman*, 1990]) are 15 K km^{-1} and 210 K, respectively [*Kieffer et al.*, 1977], and the melting point of ice is 273 K. Thus the cryosphere thickness would have been $\sim(273 - 210)/15 = 4.2$ km. Models of the outer several kilometers of the Martian crust [*Clifford*, 1993; *Hanna and Phillips*, 2003, 2005b] suggest that it may have an average pore space of $\sim$10% (Figure 6). This value would be a function of the changing state of stress in the crust caused by the emplacement of the dike that initiated the graben [*Hanna and Phillips*, 2005b], but with cryosphere compressibilities in the range 10^{-10} to 10^{-9} Pa^{-1} [*Hanna and Phillips*, 2005b], the change in porosity would be minor ($\sim$0.1% to 1%). If we assume that all of the pore space was filled with ice, and that after the ice melted and the water was lost to the atmosphere the pore space compacted to, say, 2/3 of its original value, the vertical subsidence would have been $[(1/3) \times 0.1 \times 4200 =] \sim$140 m. After the crustal heat pulse from the first dike intrusion event had been dispersed, a new cryosphere presumably developed, as a result of upward percolation of water vapor from the underlying aquifer system as it recharged. The compaction of pore space that had occurred as a result of the first event would have reduced the pore space to $\sim$6.6%. If any residual water were present in this pore space it would have frozen after dissipation of the heat from the first dike, leading to a $\sim$9% increase in volume implied by the relative densities of ice and water [*French*, 1996], possibly expanding the pore space to $\sim$7.2%. Thus the compaction that occurred after the second intrusion might have been $[(1/3) \times 0.072 \times 4200 =] \sim$101 m.

[13] We round these two estimates of thermally induced cryosphere compaction to 150 m and 100 m, respectively. Thus the amounts of graben floor lowering estimated so far

are 200 m of vertical movement along faults and 150 m of cryosphere compaction in the first event and 200 m of vertical movement along faults and 100 m of cryosphere compaction in the second event, giving a total of 650 m. The current depth of the graben floor below its rim near the gap is 750 m, and so we ascribe the remaining 100 m difference to there having been 50 m of floor erosion by the water flowing through the graben during each flood event. The floor level changes implied by this analysis are specified in Table 1; the first event is illustrated in Figure 7, and the second is illustrated in Figure 8.

[14] We now consider the implication of our inference that part of the first intruded dike is exposed as the series of $\sim$200 m high ridges on the present graben floor. It seems inevitable that the dike material, having cooled after the first event and thus being rigidly embedded in the crust forming the floor of the first graben, would have been carried down with this crust as it subsided further during the second intrusion event. Thus the present level of exposure represents the combined effects of floor lowering due to flowing water erosion and cryosphere compaction during both events. Our estimate of the total lowering by these processes during the second event was given in the previous paragraph as (100 + 50 =) $\sim$150 m. This implies that after the first event, the top of the dike was already exposed by $\sim$50 m. The total lowering by water erosion and cryosphere compaction during the first event was estimated above as (150 + 50 =) $\sim$200 m. Thus we infer that the top of the dike reached to within $\sim$150 m of the surface during the first intrusion. The tops of dikes associated with graben formation do not normally approach close to the surface [*Mastin and Pollard*, 1988; *Rubin*, 1992]. As part of a model of the formation of Martian graben by dike intrusion, *Wilson and Head* [2002] summarize work by *Rubin* [1992], who found that for a set of dike-related graben in Iceland, the ratio (graben width/depth of top of dike below surface) was $\sim$3.5. If the same ratio applies to dike-induced graben on Mars (as it should, being independent of gravity and largely controlled by rock strength), then the typical graben widths in the least modified and least complicated parts of Mangala Fossa, $\sim$2000 m, suggest that the depth to the dike top should have been about 570 m. This is substantially greater than our 150 m estimate. However, we note that there is very strong evidence [*Wilson and Head*, 2004] that a phreatomagmatic eruption took place during one (presumably therefore the first) of the intrusion events at the eastern end of Mangala Fossa, implying that the dike top was unusually shallow here, and this is consistent with the observation that the absolute heights of the tops of the dike outcrop ridges increase toward the east (Figure 4). Using *Rubin*'s [1992] data source for dikes on Earth, *Wilson and Head* [2002] found that the ratio (dike width/vertical subsidence of graben floor) was equal to $\sim$1.25. The $\sim$400 m

Table 1. Values Deduced for Floor Level Changes During the Two Episodes of Dike Intrusion and Water Release

|	First Event	Second Event
Vertical graben subsidence	200 m	200 m
Floor erosion by flowing water	50 m	50 m
Subsidence due to cryosphere ice melting	150 m	100 m
Total lowering of floor level	400 m	350 m
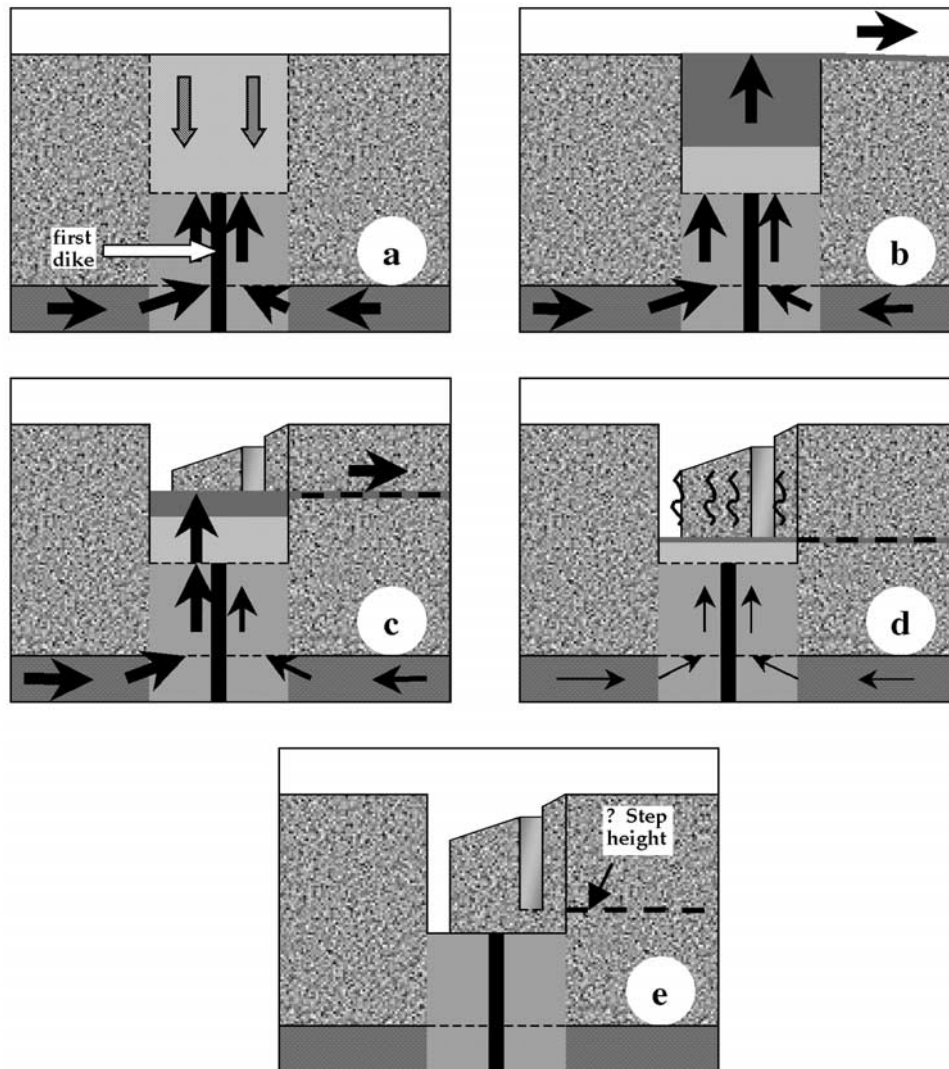
Figure 7. Proposed dike-induced formation of Mangala Fossa and evolution of first flood event. Not to scale. Look is to the west. North is to the right. (a) Emplacement of first dike from Arsia Mons causes fracturing of the surrounding aquifer and cryosphere. Thawing, subsidence, and collapse of the cryosphere above and around the hot magma in the dike begins. Water is released from the pressurized aquifer below. (Arrow size represents water quantity). (b) The graben at Mangala is formed and fills with water up to a depth of ~200 m, which spills over the graben rim. The main outflow is over the lowest part of the north rim. (c) This part of the north rim is eroded down by the outflow of water, forming a gap, which is ~5 km in width. Lateral water flow within the graben erodes its floor by ~50 m. (d) The amount of water released from the aquifer now decreases, and erosion of the gap and the floor stops, as the amount of water released is now less than the amount of water escaping into the atmosphere. This ponded water would likely be ice covered and would sublimate. (e) Heat from the cooling dike melts cryosphere ice to form water which sublimates, causing floor subsidence of ~150 m. Eventually, any residual water in the fractured cryosphere freezes.

total depth of fault-related graben floor subsidence then suggests that the sum of the widths of the two dikes should be ~500 m. This appears to be consistent with the ~270 m width of the first dike deduced from the images (Figure 5) and implies that the second dike was ~230 m wide. These widths lie well within the range deduced by *Wilson and Head* [2002] for intrusions in giant dike swarms on Mars, and are comparable to the measured widths of analogous giant dikes on Earth [*Ernst et al.*, 1995].

[15] These estimates of the dike widths allow us to verify a tacit assumption in the above treatment of graben floor lowering by cryosphere compaction after ice melting, which is that enough heat was released from each dike to melt the ice in the whole of the cryosphere forming the floor of the graben. We note that heat release will have been aided by the en echelon nature of the dike emplacement which will have placed a greater surface area of the dike in contact with the cryosphere [*Leask*, 2005]. We calculate the total amount of sensible heat released by a dike 250 m thick cooling from an initial temperature of 1450 K (we assume that the dike was mafic) to some equilibrium temperature which is also taken to be the temperature of both the water and the rock
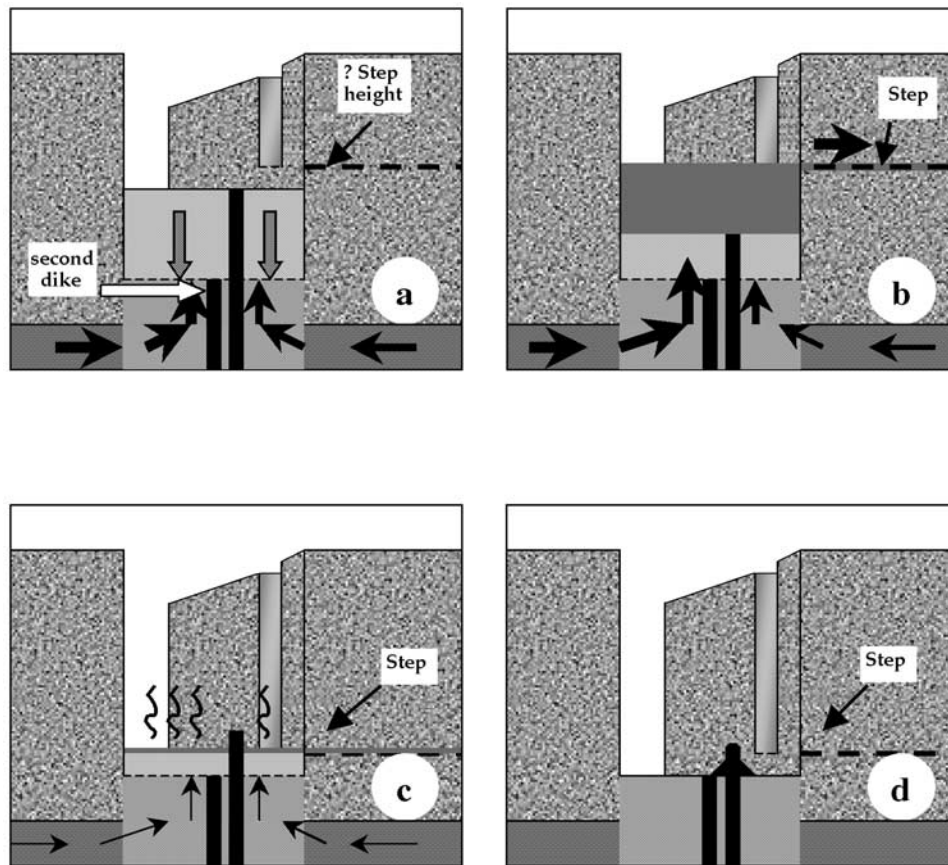
Figure 8. Proposed evolution of second flood event related to second dike intrusion in Mangala Fossa. Not to scale. Look is to the west. North is to the right. (a) Emplacement of second dike from Arsia Mons causes more fracturing of the surrounding aquifer and cryosphere. Mangala Fossa is widened and deepened further. Thawing, subsidence, and collapse of the cryosphere above and around the hot magma in the dike begins. Water is released from the recharged pressurized aquifer below. (Arrow size represents water quantity). (b) The graben fills with water up to an estimated depth of ~387 m (estimated height of the step is shown). This leads to further erosion and deepening of the gap (by ~400 m) and of the graben floor (by ~50 m). Part of the top of the first dike is left exposed above the graben floor. (c) The amount of water released from the aquifer now decreases, and erosion of the gap stops, as the amount of water released is now less than the amount of water escaping into the atmosphere. This ponded water would likely be ice covered and would sublimate. (d) Heat from the cooling dike melts cryosphere ice to form water which sublimates, causing floor subsidence of ~100 m. Eventually, any residual water in the fractured cryosphere freezes. The estimated present height of the step above the adjacent graben floor is between 45 m and 165 m. Weathering of part of the top of the first dike above the graben floor continues.

components after cryosphere ice melting has occurred in the remaining 1750 m width of a zone 2 km wide. This zone is heated by a mixture of convection [*Ogawa et al.*, 2003] in the water component (assumed to be 10% of the volume on the basis of the *Hanna and Phillips* [2003, 2005b] models) and conduction through the rock component (the remaining 90% of the volume). This calculation is approximate because it neglects any latent heat of crystallization released by the magma and assumes that all of the available heat is confined to a zone with the width of the graben floor, whereas some of this heat may well be convected beyond this zone. However, these two processes will tend to compensate for one another. The material properties used are densities of 917 kg m^{-3} for ice, 1000 kg m^{-3} for water, and 3000 kg m^{-3} for both cryosphere rock and magma; specific heats of 2000 J kg^{-1} K^{-1} for ice, 4190 J kg^{-1} K^{-1}

for water, and 1000 J kg^{-1} K^{-1} for rock; and latent heats of 3.33 × 10^5 J kg^{-1} for ice melting and 2.5 × 10^6 J kg^{-1} for water evaporation. The initial mean temperature of the cryosphere is taken as 241.5 K, the average of the surface temperature, 210 K, at the top and the ice melting point, 273 K, at the base. The heat required to warm the cryosphere ice and rock from this mean temperature to the point where ice has finished melting everywhere but the temperature has not risen above 273 K is then 8.92 × 10^{14} J per meter along strike of the dike. The vertical extent of the dike is 4050 m (recall that it intrudes to within 150 m of the surface of the 4200 m thick cryosphere) and its width is ~250 m. To liberate the above amount of heat the dike magma would only have to cool by ~294 K, so clearly there is more than enough heat to melt all of the ice. The additional amount of heat required to raise the temperature of the water fluid in the

Table 2. Variation of Water Rise Speed U, Water Volume Flux V, Water Transit Time τ, Amount of Water Cooling δT_a, and Water Release Temperature T_r as a Function of Fracture Width W[a]

W, m	U, m s^{-1}	V, m^3 s^{-1}	Re	τ, s	δT, K	T_r, °C
0.13	4.7	1.25×10^5	3.8×10^6	891	40.6	2.9
0.20	5.9	2.50×10^5	7.6×10^6	707	22.8	20.7
0.32	7.5	5.00×10^5	1.5×10^7	561	12.8	30.7
0.51	9.4	1.00×10^6	3.0×10^7	445	7.2	36.3
0.80	11.9	2.00×10^6	6.0×10^7	354	4.0	39.5
1.05	13.6	3.00×10^6	9.0×10^7	309	2.9	40.6
1.48	16.1	5.00×10^6	1.5×10^8	261	1.9	41.6
2.34	20.3	1.00×10^7	3.0×10^8	207	1.1	42.4
2.65	21.6	1.20×10^7	3.6×10^8	195	0.9	42.6

[a]The corresponding Reynolds number, Re, is given to justify the use of equation (3).

cryosphere above its boiling point, $\sim 2.4 \times 10^6$ J kg^{-1} [*Kaye and Laby*, 1966], is almost independent of the pressure distribution with depth and corresponds to $\sim 1.69 \times 10^{15}$ J per meter along strike. The amount by which the magma would have to cool to provide this additional heat is a further 556 K, bringing the magma temperature down to (1450 − 294 − 556 =) ~ 600 K. A more complicated recursive calculation, which accounts for the heat required to raise the temperatures of both the rock and water components of the cryosphere above the ice melting point, shows that the average maximum temperature that would have been reached is ~ 310 K, with the H_2O being a vapor at shallow depths and a liquid at greater depths. We stress the word average here, because the highest temperatures would inevitably be reached closest to the dike.

4. Transport of Water to the Surface

[16] In section 3 we estimated the cryosphere thickness at the time of the formation of Mangala Fossa to be ~ 4.2 km. Models of the compaction of the Martian crust [*Clifford*, 1993; *Hanna and Phillips*, 2003, 2005b] (Figure 6) suggest that the aquifer system extended from the base of the cryosphere to a depth of ~ 10 km, below which porosity decreased rapidly. This would make the aquifer thickness $\sim (10 - 4.2 =)$ 5.8 km and the increase in temperature across it $\sim (5.8 \times 15 =)$ 87 K. Thus the temperature at the base of the aquifer would have been ~ 360 K (87°C) and the mean temperature of the aquifer water, mixed by thermal convection, would have been $\sim (273 + 360)/2 = 316.5$ K (43.5°C). To estimate how much cooling might have occurred during transport of water to the surface we need to consider the motion of the water in the fracture.

[17] The graben boundary fracture permitting water flow from the subcryosphere aquifer to the surface is treated as a planar, parallel-sided fissure having a vertical length H of 4.2 km (the thickness of the cryosphere calculated in section 3), a horizontal length L (which is assumed to be equal to the 210 km length of the graben) and a width W. It is assumed that water is driven up the fracture by the pressure due to a head of water controlled by the regional topography. However, we note that an alternative pressure source could be the change in stress state of the rocks in the region of the graben due to the injection of the dike, as modeled by *Hanna and Phillips* [2005b]. The part of Mangala Fossa acting as the source of Mangala Valles is a low point on the strike of the graben (Figures 1 and 4) with higher ground to the west, east and south. If the pressure source is topographic, the controlling elevation difference is probably that to the east with a value of ~ 2 km. The excess aquifer pressure implied by this is $\sim (2000$ m $\times 3.72$ m s$^{-2} \times 1000$ kg m^{-3} =) 7.4 MPa and so the pressure gradient driving water up the fracture, dP/dz, is $(7.4 \times 10^6$ Pa)/(4200 m =) 1760 Pa m^{-1}. In their tectonic model, *Hanna and Phillips* [2005b] find an excess pressure of ~ 10 MPa, and this would imply a similar pressure gradient to that used here. The speed U of the water in the fracture, assuming its motion to be turbulent, is then given by

$$U = [(W \, dP/dz)/(f \, \rho)]^{1/2}, \tag{1}$$

where f is a wall friction factor of order 10^{-2} and ρ is the water density. For a series of values of W, Table 2 shows the corresponding variations of U and the volume flux V equal to (UWL). Also shown is the corresponding Reynolds number, $Re = (2 \, U \, \rho \, W)/\eta$, where η is the water viscosity, about 6.3×10^{-4} Pa s at the initial water temperature $T_w = 43.5$°C, and the transit time, τ, required for a given batch of water to flow up through the fracture. All the values of Re are much greater than 2000, thus verifying that the use of equation (1) for turbulent flow is justified.

[18] The transit time τ is important in that it controls the amount of heat lost by the water. At a time t after the opening of the fracture, a wave of warming will have penetrated a distance λ into the surrounding crust given by $(\kappa \, t)^{1/2}$, where κ is the thermal diffusivity of the cryosphere material, about 7×10^{-7} m^2 s^{-1}. The crustal temperature gradient controlling heat flow away from the fracture will then be dT/d$x = (T_w − T_c)/\lambda$, where T_c is the mean cryosphere temperature. The total heat flux out of the two faces of the fracture is $(2 \, k \, H \, L \, dT/dx)$, where k is the thermal conductivity of the cryosphere, about 2 W m^{-1} K^{-1}, and so the heat lost during the transit time τ will be $(2 \, \tau \, k \, H \, L \, dT/dx)$. The mass of water losing this heat is equal to $(\rho \, W \, L \, H \, s)$, where s is the specific heat of the water, about 4180 J kg^{-1}, and so the temperature decrease in the water will be $\delta T = (2 \, \tau \, k \, H \, L \, dT/dx)/(\rho \, W \, L \, H \, s) = (2 \, \tau \, k \, dT/dx)/(\rho \, W \, s) = [2 \, \tau \, k \, (T_w − T_c)]/[\rho \, W \, s \, (\kappa \, t)^{1/2}]$. This formula implies that the cooling is infinitely large at zero time, so it is appropriate to find the average value of δT over the travel time τ, of a given batch of water through the fracture. This is given by $\delta T_a = (1/\tau) \int \delta T(t) \, dt$, and for the first batch of water rising through the fracture, for which heat loss is at a maximum because there has not yet been any heating of the fracture walls, the integral is to be evaluated between $t = 0$ and $t = \tau$, and is found to be $[4 \, \tau^{1/2} \, k \, (T_w − T_c)]/[\rho \, W s \, \kappa^{1/2}]$. Table 2 shows these values of δT_a, together with the actual water release temperatures, T_r, that they would produce if, as estimated earlier, the initial water temperature in the aquifer were 43.5°C. Clearly, cooling during transport of water to the surface would only be significant for fractures narrower than ~ 0.3 m, corresponding to a water flux of $\sim 5 \times 10^5$ m^3 s^{-1}, and would be critical for fractures narrower than ~ 0.1 m. Table 2 contains information for water fluxes up to a little more than 10^7 m^3 s^{-1}, because the maximum water flux through the Mangala Valles channel system was probably of this order [*Komar*, 1979; *Ghatan et al.*, 2004; *Leask*, 2005]. The fracture width required to deliver this flux is ~ 2.3 m and the water flow speed is ~ 20 m s^{-1}.

Table 3. Variation of Water Fountain Height H_f, Fountain Width W_f, Initial Water Flow Speed Across the Graben Floor S, Initial Water Depth Y, Water Flow Speed S_j and Depth Y_j After Passing Through a Hydraulic Jump, Distance That Water Could Flow Across the Floor Before Cooling to the Freezing Point, d_f, Maximum Thicknesses of Ice Layers Forming on the Water When the Water Must Spread 1 and 2 km, X_1 and X_2, Respectively, Corresponding Timescales for Completion of Floor Flooding τ_{f1} and τ_{f2}, and Net Graben Filling Rate After Floor is Flooded, Y', as a Function of Water Volume Flux V

V, m^3 s^{-1}	H_f, m	W_f, m	S, m s^{-1}	Y, m	S_j, m s^{-1}	Y_j, m	d_f, m	X_1, mm	X_2, mm	τ_{f1}, s	τ_{f2}, s	Y', mm s^{-1}
1.25×10^5	3.0	0.25	4.7	0.13	0.52	1.18	65	11	23	1923	3846	−0.14
2.50×10^5	4.7	0.40	5.9	0.20	0.64	1.84	180	10	22	1563	3125	−1.27
5.00×10^5	7.5	0.64	7.5	0.32	0.81	2.95	373	8	20	1235	2469	−2.61
1.00×10^6	11.9	1.01	9.4	0.51	1.03	4.67	745	3	15	971	1942	−2.98
2.00×10^6	19.0	1.60	11.9	0.80	1.28	7.41	1479	0	6	781	1563	−1.67
3.00×10^6	24.9	2.10	13.6	1.05	1.47	9.71	2217	0	0	680	1361	0.28
5.00×10^6	34.9	2.95	16.1	1.48	1.75	13.64	3699	0	0	571	1132	4.65
1.00×10^7	55.5	4.69	20.3	2.34	2.20	21.63	7370	0	0	455	909	16.22
1.20×10^7	62.6	5.29	21.6	2.65	2.34	24.49	8881	0	0	427	855	20.92

[19] The approximate timescale for the development of the water flow regime can be estimated as follows. At any point along the graben the initial fracture would have formed as a result of the stresses initiated by the intrusion of the dike. The part of the graben acting as the source of the Mangala Valles is about 2000 km from the magma source under Arsia Mons. Models of the propagation of giant dikes fed directly from mantle plume heads on Mars [*Wilson and Head*, 2002] show that at this distance, the dike propagation speed would have been of order 10 m s^{-1}. The radius of curvature of the dike tip would be about half the dike height, say ~30 km, and so the time for the dike width to have become fully developed would have been ~(30,000 m)/ (10 m s^{-1}) = ~3000 s. The graben fracture precursors would form quickly once the stresses due to the dike injection were large enough to initiate them; to break 4.2 km of cryosphere rock at about half of the speed of sound in rock, say 1 km s^{-1}, takes ~4 s. However, it is hard to estimate how long it would have taken before the stresses became large enough to start fractures propagating. We arbitrarily assume that it took two thirds of the ~3000 s dike width development time, so the remaining ~1000 s was the time taken by the graben floor to subside to a depth of 200 m, implying a subsidence speed of ~0.2 m s^{-1}. The time for the water flow to develop in the aquifer was the aquifer length, ~1000 km [*Leask*, 2005] divided by the speed of sound in water, ~1.4 km s^{-1}, i.e., ~700 s. The time required for water to flow up the 4.2 km long cryosphere fracture, at a speed that Table 2 shows to be initially ~14 m s^{-1}, was ~300 s. Thus water first started to emerge into the graben ~300 s after the graben boundary faults formed and subsidence started, and the development of the water release rate was completed ~700 s later, ~1000 s after subsidence started, which implies that the graben floor finished its descent at about the time the full water flow rate was reached.

[20] The above analysis (and that which follows) is predicated on the assumption that the pressure gradient driving water up the fracture did not change significantly over at least the time needed to fill the graben, which we show in section 5 to be ~2 hours. In a detailed model coupling flow in an aquifer to discharge through a fracture allowing water to escape to the surface, *Manga* [2004] has shown that after a rapid rise to a maximum value, the discharge should decrease in a way dictated by the permeability of the aquifer. For the aquifer-fracture system at

Cerberus Fossae feeding the Athabasca Valles channel system, *Manga* [2004] found a discharge decay timescale of ~0.5 hours if the permeability of the Martian aquifer was comparable to that of basaltic lava flows on Earth, ~10^{-9} m^2. Since permeabilities of many terrestrial crustal rocks are commonly very much smaller than those of relatively fresh lavas, this can be taken to imply that longer timescales would not be expected on Mars. If the discharge decay timescale were indeed ~0.5 hours, all of our timescale estimates above would have to be increased by at least a factor of ten if we retained the same peak discharge of ~10^7 m^3 s^{-1}; alternatively an order of magnitude larger peak discharge would have to be invoked.

[21] This comparison underlines a major issue. The various analyses implying that water discharges of ~10^7 m^3 s^{-1} are needed to form the Mangala Valles [*Komar*, 1979; *Ghatan et al.*, 2005; *Leask*, 2005] also imply that something approaching this level of discharge must be maintained for up to 2 months, not a few hours [*Tanaka and Chapman*, 1990; *Dohm et al.*, 2001a; *Fuller and Head*, 2002b; *Leask*, 2005]. Analyses of other Martian outflow channel systems have invoked even larger peak discharges, at least ~10^8 and possibly ~10^9 m^3 s^{-1} [*Robinson and Tanaka*, 1990; *Ori and Mosangini*, 1998; *Dohm et al.*, 2001b]. *Wilson et al.* [2004a] pointed out that given our current understanding, these rates could not be sustained for even a few minutes unless Martian aquifers were 2 orders of magnitude more permeable than expected based on terrestrial comparisons. This issue is very far from being resolved, but we feel justified in proceeding on the assumption that a discharge of ~10^7 m^3 s^{-1} can be maintained for at least many hours.

5. Behavior of Water Filling the Graben

[22] When the water flowing up either or both of the graben bounding fractures reached the surface its velocity must have carried it up to form a fountain from which it descended again to feed a surface flow spreading away from the fracture toward the center of the graben. Conservation of mass and energy then require that on average, the lateral speed of the water, S, was equal to the speed at which it flowed up the fracture, and that the initial depth of the water, Y, was equal to the fracture width. These values, together with the implied fountain heights, H_f, and widths, W_f, are shown in Table 3 as a function of the water volume flux taken from Table 2. At the onset of water release the

fountain must have been at least ~25 m high and ~2 m wide. This small width is consistent with the lack of any surface features close to either rim of the graben that might provide evidence of this kind of activity irrespective of whether any significant water release had occurred before much of the 200 m of graben subsidence had taken place. The values of S and Y in Table 3 show that the initial Froude number, F_i, of the water flowing away from the fracture, equal to $S/(g\,Y)^{1/2}$, was close to ~6.9 (independently of the water volume flux), implying that the flow was supercritical and that a hydraulic jump would have very quickly taken place to reduce the flow to a subcritical state. The factor ϕ by which the depth would increase and the speed would decrease was found from F_i using the standard relationship [e.g., *Chow*, 1959] $\phi = 0.5\,((1 + 8\,F_i^2)^{1/2} - 1)$ to be ~9.2, leading to a Froude number after the jump of ~0.25.

[23] Once released, the water must also have begun to evaporate. Using an annually averaged atmospheric model for Mars to estimate the atmospheric pressure at the level of the graben floor as it subsided we find an average value during the first subsidence event of 602 Pa. This implies that the vapor pressure of the water was greater than the atmospheric pressure at all temperatures above the freezing point. Under these conditions, the evaporation rate will have depended only on the difference between the vapor pressure and the atmospheric pressure [*Wallace and Sagan*, 1979]. The mass of water vapor per unit area per second being lost from the water surface at any given temperature can then be calculated using formulae given by *Hecht* [1990, p 297]. Dividing the mass flux per unit area by the density of the water, ~1000 kg m^{-3}, gives the speed at which the spreading water layer gets shallower. Multiplying the mass flux per unit area by the latent heat of evaporation, close to 2.4×10^6 J kg^{-1} at all temperatures of interest here, gives the heat flux per unit area leaving the flow, and dividing the heat flux by the product of the density, specific heat (~4190 J kg^{-1} K^{-1}) and depth of the water gives the rate at which the water temperature decreases with time. Dividing the water depth by the rate of shallowing gives an estimate of the time before all of the water has evaporated, and multiplying this time by the lateral water flow speed gives the distance that water can travel before this occurs. This distance is found to be much greater than the graben width for all water release rates of interest here and is not a limitation on the initial graben flooding. Finally, dividing the initial release temperature in °C by the cooling rate gives an estimate of the time before the water begins to freeze, and multiplying this time by the lateral water flow speed gives the distance, d_f, that it can travel before starting to freeze. In detail, neither the rate of shallowing nor the rate of cooling are constant because the evaporation rate is temperature-dependent, and so the depth and temperature changes described above were evaluated numerically by recalculating the rates as the temperature changed.

[24] The results are given in Table 3. If only one boundary fault releases water, ice formation is avoided for all water release rates greater than ~3×10^6 m^3 s^{-1}, and if both faults are active, ice formation is avoided if the flux up each fault is greater than ~2×10^6 m^3 s^{-1}, i.e., a total flux of >4×10^6 m^3 s^{-1}. For all smaller discharge rates some ice formation occurs. The maximum amount of ice that forms can be found by dividing the time available to form ice

by the time needed to freeze all of the water once it has reached 0°C. The time available for ice formation is equal to the difference between the distance that has been traveled by the water when the freezing point is reached and the total distance that must be traveled (over most of the length of the graben this is 2 km if only one fault releases water and 1 km if both do so) divided by the lateral water flow speed. The time that would be needed to freeze all of the water is equal to the product of the water depth, water density and latent heat of fusion divided by the heat loss rate per unit surface area at the freezing point. The ratio of these two times gives the fraction of the depth of the laterally spreading water that freezes, and this fraction multiplied by the water depth gives the thickness of the resulting ice layer, assuming that all of the crystals float to the surface of the water. Table 3 shows the maximum ice depths for the 1 km distance, X_1, when both boundary faults release water, and for the 2 km distance, X_2, when only one does so. The corresponding times, τ_{f1} and τ_{f2}, needed to complete the floor flooding are also shown. It seems unlikely that more than ~20 mm thickness of ice formed during the floor flooding process along most of the graben. However, near the gap, where the graben is wider, up to twice this thickness might be formed. We note that all of the above calculations of ice production rate would change if the atmospheric pressure were significantly different from the 602 Pa annual average value adopted. Lower pressures would not cause a great change, because the evaporation and heat loss rates would still be dominated by the vapor pressure of the water, but pressures much higher than ~610 Pa, the water vapor pressure at the triple point, would cause a drastic reduction in evaporation and heat loss rates [*Wallace and Sagan*, 1979], probably completely precluding ice formation.

[25] Taken together, the various constraints outlined so far on the water release processes suggest that the earliest flows up the fracture(s) took place at discharge rates in excess of ~1.5×10^5 m^3 s^{-1}, implying fracture widths of at least 0.15 m, and grew steadily to a maximum value of ~10^7 m^3 s^{-1} over a 700 s interval, which Table 3 shows is comparable to the time taken to completely flood the graben floor. The subsequent net filling rate, Y', the amount by which the depth increase rate due to the inflow exceeded the depth reduction rate due to continuing evaporation, is shown in Table 3 for each total water release rate. It becomes positive for inflow rates greater than ~3×10^6 m^3 s^{-1}. A period of ~100 seconds was needed for the water inflow rate to increase from ~5×10^5 m^3 s^{-1} to 3×10^6 m^3 s^{-1}, during which time the water motion on the floor of the graben would have been complex as the initial surge settled into a more ordered subcritical flow. If the water was not well mixed during this period it is possible that at least another ~5 mm of ice formation took place. During the next ~250 s the water flux increased from 3×10^6 m^3 s^{-1} to 1×10^7 m^3 s^{-1}. Thereafter the water inflow rate was constant at ~1×10^7 m^3 s^{-1}, though the water evaporation rate was still a function of the surface water temperature.

[26] There are two possible extremes for the behavior during this period. If all of the water was well mixed, its average temperature can be found by a simple heat-sharing calculation, and the results of this are shown in Figure 9. Filling of the graben to its 200 m depth would have occurred ~9055 s (~2.5 hours) after floor flooding was
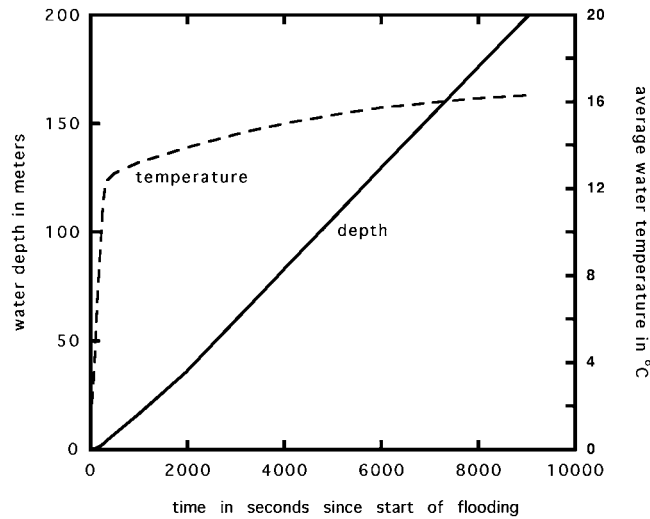
Figure 9. Variation with time since start of water release during first release event of (left side) water depth in graben and (right side) average water temperature.

complete and the water temperature would have been ~16°C. The other extreme possibility is that the water was not well mixed but instead became stratified as its depth increased. In that case the surface would have cooled rapidly and an ice layer would have developed all over it. The deeper water would have quickly reached the temperature at which water was being released from the fracture, ~42°C, and a thermal boundary layer would have separated the ice from the warm water. The surface of the ice would have cooled to the ambient temperature, ~210 K, and the thickness of the ice layer, Z, as a function of time, t, can be predicted by equating the heat flux through the ice layer to the latent heat of freezing extracted from the water just below it, giving

$$Z = [(2\,C\,\Delta T)/(\Lambda\,\rho_i)]^{1/2}\,t^{1/2}, \qquad (2)$$

where ΔT is the temperature difference across the layer, $\sim(273 - 210 =)$ 63 K, C is the thermal conductivity of ice averaged over the 273–210 K range, ~2.5 W m^{-1} K^{-1}, Λ is the latent heat of freezing, 3.33×10^5 J kg^{-1}, and ρ_i is the ice density, ~917 kg m^{-3}. Because the surface of the ice is at the low ambient temperature, the rate of depth reduction of the ice layer by evaporation is very small [*Wallace and Sagan*, 1979] and can be neglected, and so the graben filling rate is greater than in the case of the open water surface; the graben fills to its 200 m depth in ~8560 s and the ice thickness reaches ~94 mm. This must be a maximum estimate, because it assumes that the ice layer is uniform and stable over all of the water surface. During the first ~1000 s of the ~8560 s, graben subsidence will still have been taking place, and so some local movement of water along the axis of the graben would almost certainly have taken place, disturbing the water surface.

[27] So far in this section we have assumed that the width of the fracture and the corresponding water discharge rate were controlled entirely by the pressure distribution in the aquifer system. However, it is possible that the initial fracture was widened, at least in part, by the relatively warmer water thermally eroding its cold walls. In that case it could well have taken longer than we have calculated to reach the peak discharge rate, and so the graben would have taken longer to fill; indeed, if the erosion timescale were more than ~1 hour, the graben would have become full before the peak discharge rate was reached. A second consequence of a slower filling rate is that the likelihood of stratification of the water in the graben is increased, encouraging ice formation on the water surface, and the longer filling time allows a greater ice thickness to develop, equation (2) showing that the thickness is proportional to the square root of the time. As an extreme example of these issues, we consider a case where the fracture opens rapidly through the cryosphere, during dike emplacement, to a width of ~0.3 m and is then widened to ~2.3 m (consistent with the final ~10^7 m^3 s^{-1} water discharge rate) by a 1 m erosion of each of its walls as a thermal wave melts cryosphere ice. As discussed in section 4, the penetration distance in time t is $(\kappa\,t)^{1/2}$ and with $\kappa = \sim7 \times 10^{-7}$ m^2 s^{-1}, the time required is $\sim1.4 \times 10^6$ s or ~17 days. Published models of the formation of the Mangala Valles [*Tanaka and Chapman*, 1990; *Dohm et al.*, 2001a; *Fuller and Head*, 2002b] suggest 1 to 2 months for the duration of the event, and ~17 days is a very much larger fraction of this duration than the ~1 hour proposed earlier, but it cannot be excluded by the available evidence. In this extreme case, the ice thickness on the water overflowing the graben could have been as much as 1.2 m.

6. Water Flow out of the Graben

[28] The present average width of the gap in the north wall of the graben is ~5.5 km, and it seems clear from the geometry of the gap and the adjacent channels that the bulk of the water leaving the graben in the first flood event (and all of the water in the second event) utilized this escape route. It seems reasonable to assume that the initial overflow began at the absolutely lowest point on the wall and spread both eastward and westward as the overspilling water depth increased until equilibrium was reached. The width of this overflow region is estimated to have been ~7.0 km, based on measuring the distance between the tops of the cliffs defining the gap where they border the graben. The depth of water in the center of the overspill can be estimated from the observation that the downward slopes of the north graben wall toward the gap are 0.0165 from the west and 0.0108 from the east. Taking the average of these slopes, say 0.0136, and the 3500 m half width of the gap, the depth of water in the center of the overspill would have been (0.0136 × 3500) = ~47.6 m. The initial cross-sectional shape of the overspill was then an inverted isosceles triangle ~7.0 km wide and ~47.6 m deep; this corresponds to a cross-sectional area of ~167,000 m^2 and an average depth of ~23.8 m. The northward slope, α, of the ground at the location of the gap was estimated by examining the present-day slope of the ground on either side of the gap as sin $\alpha = 0.058$ by *Ghatan et al.* [2005]. In section 2 we noted evidence for some limited water escape over the rim of the graben in a few other places, especially two locations on the south side to the east of the gap which connect to the low-lying interior of an old eroded crater [*Head et al.*, 2004]. The total horizontal extent of these additional zones

of water escape is ~5 to 6 km. For modeling purposes we make what we consider to be the reasonable assumption that these locations had similar average depression depths and ground slopes to those of the protogap, and hence infer that the initial escape of water from the graben took place through the equivalent of a ~12.5 km wide, ~23.8 m deep channel with a floor slope of 0.058.

[29] This initial water flow would have taken place in accordance with the classical treatment of flow in open channels which, using the Darcy-Weisbach equation in preference to the Manning formula [*Wilson et al.*, 2004a], gives the mean flow speed, U_c, as

$$U_c = [(8\, g\, R \sin \alpha)/f_c]^{1/2}, \qquad (3)$$

where R is the hydraulic radius of the water channel, essentially equal to the ~26 m depth of the flow, sin α is 0.058, and f_c is the Darcy-Weisbach friction factor. The value of the bed friction factor for this water depth, $f_c =$ ~0.0335, is found by combining estimates of the typical sizes of rocks at the Viking and Pathfinder landing sites with empirical data on the effects of bed roughness on water flow in channels on Earth as described by *Wilson et al.* [2004a]. The resulting mean water speed is 36.4 m s^{-1}, and multiplying this by the mean water depth and the ~12.5 km total width of the flowing water implies a maximum initial discharge from the graben of ~1.08×10^7 m^3 s^{-1}. This discharge is almost exactly equal to the 1×10^7 m^3 s^{-1} rate at which water was filling the graben in our standard scenario in which the discharge rate is reached rapidly after the dike is emplaced, and implies that between them, the three initial main overflow locations were almost certainly able to accommodate all of the water. They would certainly have been able to do so if the increasing rate of water supply had been controlled by thermal erosion of the fracture, as described at the end of section 5, so that the peak discharge of 1×10^7 m^3 s^{-1} was not reached until long after the graben was full.

[30] As soon as water began to flow through the notches in the wall, downcutting of their floors by erosion would have begun. It is clear from the present geometry that this was minimal in the notches on the south rim, and that the notch in the north wall where the present gap is located was almost immediately dominant in draining water. The depth of the gap at the end of the first erosion event was found in section 3 to have been ~250 m, and estimates of the duration of the main flood forming the Mangala Valles range from ~10 days to ~2 months [*Tanaka and Chapman*, 1990; *Dohm et al.*, 2001a; *Fuller and Head*, 2002b; *Leask*, 2005]. If a duration of, say, one month is assumed as the time taken to erode the 250 m depth of the gap, the erosion rate implied is just less than 100 μm s^{-1}. This rate is comparable to that estimated (~50 m in 2 weeks = ~40 × 10^{-6} m s^{-1}) for the erosion of the channeled scabland by the Missoula flood on Earth, the most commonly cited terrestrial analog to Martian outflow channels [*Baker*, 1978]. Every meter of downcutting in the gap must have drained a volume equal to that one meter multiplied by the horizontal cross-sectional area of the graben which, given the 210 km length and ~2 km width, is ~420 km^2. Thus the additional discharge rate through the gap due to drainage of the graben would have been (420 km^2 × 0.1 mm s^{-1}) =

~4.2×10^4 m^3 s^{-1}. This value is only ~0.4% of the 1×10^7 m^3 s^{-1} inflow from the aquifer and so has little bearing on the history of the system.

7. Erosion of the Graben Floor

[31] The mean water flow speed along the floor of the graben can be estimated as follows. The erosion rate of the gap was ~100 μm s^{-1}, with a mean water flow speed of 36.4 m s^{-1}. By the time that erosion of its floor had deepened the gap to 35.4 m it was just able to cope with the 1×10^7 m^3 s^{-1} water flux, and so the water depth in the graben at that time would have been equal to the 200 m depth of the graben. Assume that half of the water flowed toward the gap from each of the western and eastern ends of the graben; then the flux in each half, 0.5×10^7 m^3 s^{-1}, must have been equal to the cross−sectional area of the graben, (200 × 2000 =) 4×10^5 m^2, multiplied by the mean flow speed, making the mean flow speed (0.5 × 107/4 × 105 =) 12.5 m s^{-1}. We assume that the material forming the graben floor was similar to that forming the floor of the gap. We further assume that the erosion rate of the graben floor can be found by scaling the 100 μm s^{-1} estimate for the gap given in section 6. The scaling factor will be the ratio of the velocities of water flowing across the floor and through the gap if the erosion process is momentum dominated, or will be the square of the velocity ratio if erosion is energy dominated. The implied erosion rates are then either 34.3 or 11.8 μm s^{-1}, and in the estimated one month duration of the flood event the amount of erosion will be either ~89 or ~31 m. These values are sufficiently close to the 50 m estimate derived in section 3 from the morphology that we consider that estimate to be of at least the correct order of magnitude.

[32] The surface area of the graben is ~210 km × ~2000 m = ~41×10^7 m^2, and if ~50 m of floor material was eroded in each of the two flood events the total volume removed is 42 km^3. *Ghatan et al.* [2005] estimate that the total volume of crustal material eroded to form the Mangala Valles system was ~13,000 to 20,000 km^3. Thus the volume of graben floor material was a negligible fraction of the total transported by water in the channel system. The erosion of the graben floor is important in another respect, however; it caused much or all of the evidence for any juvenile magma having been erupted onto the graben floor as lava flows to be washed away.

8. Postflood Subsidence of the Graben Floor

[33] In section 3 we estimated that the widths of the dikes causing graben subsidence at Mangala Fossa were ~270 m in the first event and ~230 m in the second, and that the dikes may have penetrated through the ~4.2 km thick cryosphere to within ~150 m of the surface. Using the average dike width of 250 m, and taking the extent of penetration to 4000 m, this implies that for each meter along strike, 10^6 m^3 of magma was intruded into the cryosphere. Assuming a plausible mafic magma temperature of 1350 K, density of 2800 kg m^{-3}, and specific heat of ~1000 J kg^{-1} K^{-1}, the amount of heat released by this magma in cooling to the melting point of ice was ~3.0×10^{15} J.

[34] This may be compared with the amount of heat required to melt all of the ice present in the cryosphere

beneath the graben floor. In section 3 we assumed that 10% by volume of the cryosphere was ice. The density of ice is $\sim$917 kg m^{-3} and its latent heat of fusion is $\sim$3.33 $\times$ 10^5 J kg^{-1}. Its average specific heat over the 273 to 210 K temperature range that spans the cryosphere is $\sim$1900 J kg^{-1} K^{-1}, with the average temperature rise to reach the melting point being $\sim$31.5 K. Thus, for each meter along strike, to warm and melt all of the cryosphere ice in a typical 2 km wide part of the graben requires $\sim$3.0 $\times$ 10^{14} J, only one tenth of the amount of heat available from the cooling dike. This implies that even allowing for the fact that the transfer of heat from the cooling dike to the more distal parts of the ice must have been relatively inefficient, despite the assistance of a hydrothermal convection system [*Gulick*, 1998; *Ogawa et al.*, 2003], we see no problem with justifying the proposal in section 3 that late stage graben floor subsidence amounts of up to 150 m were caused by this mechanism.

[35] The volume of water produced by one dike extending for the full $\sim$210 km length of Mangala Fossa and melting all the ice in a 2 km wide zone of the 4.2-km-thick cryosphere would have been $\sim$176 km^3. This is a negligible fraction of the $\sim$20,000 to 30,000 km^3 estimate by *Ghatan et al.* [2005] of the minimum total volume of water that was required to erode the Mangala Valles system. Also, the rate at which heat would have been released from the dike would have been limited by the conduction of heat from the still molten dike interior through the growing solidified layer to each subvertical interface with the host rocks, the timescale for which would have been of order (h^2/κ), where h is the half width of the dike and κ is the thermal diffusivity of silicate rock. Using $\kappa = 7 \times 10^{-7}$ m^2 s^{-1} and the average value of the dike width estimates from section 3, $h = \sim$125 m, the timescale for cooling is $\sim$1000 years. This value assumes that the dike remains impermeable to the water being produced, but extensive fracturing would be needed to reduce the timescale significantly. We conclude that no significant amount of water from the melting of ice in the cryosphere contributed to the flooding of the Mangala Valles.

9. Discussion

[36] Sections 4 to 8 dealt mainly with the processes that took place during the first dike intrusion and water flood event at Mangala Fossa. Section 3 presented evidence for two such events, with Table 1 showing that the main difference inferred from the morphology was that at the end of the second event there was a smaller amount of graben floor subsidence due to melting of cryosphere ice by heat from the cooling dike. The present geometry of the gap suggests that by the end of the first event, when the gap had been eroded to a depth of $\sim$250 m, its width at the level of its floor was $\sim$5.5 km. Assuming a similar water supply rate in the second event to that in the first, overflow of water through the gap would have taken place at a fully developed water flux of $\sim$1 $\times$ 10^7 m^3 s^{-1}. If the floor of the gap still had the same slope as in the first event, $\sim$0.058, the solution of equation (3) gives the water depth as $\sim$37.3 m and the mean flow speed as 48.7 m s^{-1}. Thus, during the second period of flooding of the graben, the water level would have had to rise from the new floor level after graben subsidence,

$\sim$600 m below the original graben rim, to the level of the floor of the gap in the north wall at the end of the first flood event, estimated to have been $\sim$250 m below the original graben rim, and then a further 37.3 m to reach an equilibrium between inflow and outflow, making a total water depth of $\sim$387 m.

[37] If the pattern of development of the water supply rate up the graben boundary fault was similar in the two flood events, the time taken to reach this equilibrium can be found, using the same methods that were applied to the first event in section 5, to be $\sim$4.9 hours in the well-mixed case. In the case where the water becomes stratified as it deepens, the filling time would have been $\sim$4.6 hours and the thickness of the ice layer on the water surface would have been $\sim$130 mm. The present level of the floor of the gap is $\sim$650 m below the original graben rim; if, as estimated in section 3, the level of the floor of the gap was $\sim$250 m below the rim at the end of the first event, an additional 400 m of erosion occurred during the second event. At a similar erosion rate to the $\sim$100 μm s^{-1} estimated for the first event, this would have required $\sim$45 days.

[38] This $\sim$387 m maximum water depth in the graben during the second flood event is approaching a factor of 2 greater than the maximum water depth in the first event. This depth of water would have exerted a significant pressure, $\sim$1.4 MPa, at its base. One consequence of the presence of this head of water is to reduce, by $\sim$8%, the pressure gradient used in section 3 to drive water to the surface, thus decreasing the maximum flow rate and increasing the filling time by a similar amount for the same assumed fracture geometry. A second consequence is some alteration of the stresses and stress gradients in, especially, the north wall of the graben, especially near the gap where its horizontal north–south thickness is at a minimum. However, there is no indication from the morphology that wholesale collapse of the wall took place; rather, the formation of the walls and floor of the gap appears to have been the result of a relatively steady water erosion process.

10. Conclusions

[39] 1. Previous work has suggested on morphological grounds that two water release events occurred at Mangala Fossa to form the Mangala Valles outflow channel system. We argue that these two events were each the consequence of a dike-induced graben formation episode at Mangala Fossa, the evidence being the inferred presence of exposed outcrops of the first dike on the floor of the graben, and the need for a second dike to induce the changes that exposed parts of the first dike. A second argument for the presence of a second dike is the unusual width of the graben near the source of the channel system. By comparison with other graben in the Memnonia Fossae group we infer that the amount of graben subsidence in each event was $\sim$200 m.

[40] 2. Previous estimates of a peak water discharge rate of $\sim$10^7 m^3 s^{-1} can be understood in terms of water flow from an underlying aquifer up one or both graben boundary faults. Typical conditions would have involved a maximum water flow speed of $\sim$20 m s^{-1} up a $\sim$2.3 m wide fracture. Depending on the extent of vertical mixing of the water, this would have filled the graben to its rim in $\sim$2.4 to 2.5 hours in the first event and in 4.6 to 4.9 hours in the second event.

[41] 3. Initial overflow of the graben, as it filled during the first event, took place from the three locally lowest points on its rim, but rapidly became concentrated into a ~7 km wide and up to ~48 m deep zone on the north rim that was subsequently eroded into the present gap. The surface in the vicinity of the two short-lived overflow points on the south rim of the graben shows textures possibly related to the presence of an ice layer on the overflowing water. If ice was present, then the atmospheric pressure at the time of the first event must have been no more than ~610 Pa.

[42] 4. The ~650 m depth of the gap, combined with previous estimates of a total duration of water flow of ~2 months, implies an erosion rate of the floor of the gap of ~100 μm s^{-1}. Scaling this erosion rate to the water flow regime within the graben implies that the floor was eroded at an average rate of ~20 μm s^{-1}, resulting in ~50 m of floor erosion during each flood event.

[43] 5. The difference of ~100 m in height between the floor of the gap and the present graben floor implies that the graben floor subsided by this amount after the second flood event ceased. The most plausible explanation is desiccation and compaction of the cryosphere by heat from the second dike. It is logical to assume that similar subsidence also took place at the end of the first flood event.

[44] 6. Because dike heating during the first event would have compacted the shallowest part of the cryosphere, where pore space was greatest, less ice would have been present in the cryosphere at the start of the second event, and so the second event would have involved less subsidence than the first. An estimate of ~150 m subsidence in the first event is consistent with this argument and is also consistent with the present ~750 m total depth of the graben in the immediate vicinity of the gap in its north wall. The floor depth changes as Mangala Fossa evolved are summarized in Table 1.

[45] 7. The region around the gap in the north wall of Mangala Fossa would be an ideal location for investigation with the MARSIS radar system on the Mars Express spacecraft, since it offers the possibility of detection of one or more shallow dikes cutting the regional cryosphere, together with possible local anomalies in the vertical distribution of H_2O in the cryosphere. It may also be possible to detect vertical displacements of horizontal cryosphere structure along the graben boundary faults.

Notation

C average thermal conductivity of ice, 273–210 K, W m^{-1} K^{-1}.

F_i value of the Froude number prior to a hydraulic jump, dimensionless.

H vertical length of fracture, m.

H_f height of water fountain of water exiting fracture, m.

L horizontal length of fracture, m.

R hydraulic radius of water flow, $\approx$ water depth, m.

Re Reynolds number of water flow in fracture, dimensionless.

S speed of water flowing across graben floor, m s^{-1}.

T_c mean cryosphere temperature, K.

T_r temperature of water exiting fracture, K.

T_w temperature of water in aquifer, K.

U rise speed of water in fracture, m s^{-1}.

U_c mean water flow speed through overflow channels, m s^{-1}.

V volume flux of water rising through fracture, m^3 s^{-1}.

W width of fracture, m.

W_f width of fountain of water exiting fracture, m.

X_1 maximum thickness of ice on water flowing 1 km, m.

X_2 maximum thickness of ice on water flowing 2 km, m.

Y initial depth of water flowing across graben floor, m.

Y' net filling rate of graben, m s^{-1}.

Z thickness of ice layer on water rising to fill graben, m.

dP/dz pressure gradient driving water up fracture, Pa m^{-1}.

dT/dx temperature gradient near fracture, K m^{-1}.

f wall friction factor, dimensionless.

f_c Darcy-Weisbach friction factor for water flow, dimensionless.

h half width of dike, m.

k thermal conductivity of cryosphere, W m^{-1} K^{-1}.

ΔT temperature difference across ice layer, K.

Λ latent heat of freezing of ice, J kg^{-1}.

α slope of ground near gap in north wall of graben, degrees.

δT_a cooling of water rising through fracture, K.

η viscosity of water, Pa s.

κ thermal diffusivity of cryosphere material, m^2 s^{-1}.

λ distance penetrated by heating wave, m.

ϕ water depth increase factor through hydraulic jump, dimensionless.

ρ density of water, kg m^{-3}.

ρ_i density of ice, kg m^{-3}.

τ transit time of water through fracture, s.

τ_{f1} time to complete flooding of 1 km wide graben floor, s.

τ_{f2} time to complete flooding of 2 km wide graben floor, s.

References

Baker, V. R. (1978), Large-scale erosional and depositional features of the Channeled Scabland, in *The Channeled Scabland: A Guide to the Geomorphology of the Columbia Basin, Washington*, edited by V. R. Baker and D. Nummedal, pp. 81–115, NASA, Washington, D. C.

Baker, V. R., R. G. Strom, V. C. Gulick, J. S. Kargel, G. Komatsu, and V. S. Kale (1991), Ancient oceans, ice sheets and the hydrological cycle on Mars, *Nature*, 352, 589–594.

Berman, D. C., and W. K. Hartmann (2002), Recent fluvial, volcanic and tectonic activity on the Cerberus Plains of Mars, *Icarus*, 159(1), 1–17.

Burr, D. M., A. S. McEwen, and S. E. H. Sakimoto (2002a), Recent aqueous floods from the Cerberus Fossae, Mars, *Geophys. Res. Lett.*, 29(1), 1013, doi:10.1029/2001GL013345.

Burr, D. M., J. A. Grier, A. S. McEwen, and L. P. Keszthelyi (2002b), Repeated aqueous flooding from the Cerberus Fossae: Evidence for very recently extant, deep groundwater on Mars, *Icarus*, 159(1), 53–73.

Carr, M. H. (1979), Formation of Martian flood features by release of water from confined aquifers, *J. Geophys. Res.*, 84, 2995–3007.

Carr, M. H. (1987), Water on Mars, *Nature*, 326, 30–35.

Carr, M. H. (1996), Channels and valleys on Mars: Cold climate features formed as a result of a thickening cryosphere, *Planet. Space Sci.*, 44(11), 1411–1423.

Carr, M. H., and G. D. Clow (1981), Martian channels and valleys: Their characteristics, distribution, and age, *Icarus*, *48*(1), 91–117.

Carr, M. H., L. S. Crumpler, J. A. Cutts, R. Greeley, J. E. Guest, and H. Masursky (1977), Martian impact craters and emplacement of ejecta by surface flow, *J. Geophys. Res.*, *82*, 4055–4065.

Cattermole, P. J. (2001), *Mars: The Mystery Unfolds*, 186 pp., Terra, Tokyo.

Chapman, M. G., and K. L. Tanaka (1990), Small valleys and hydrologic history of the lower Mangala Valles region, Mars, *Proc. Lunar Planet. Sci. Conf.*, *20th*, 531–539.

Chow, V. T. (1959), *Open Channel Hydraulics*, McGraw-Hill, New York.

Clifford, S. M. (1987), Polar based melting on Mars, *J. Geophys. Res.*, *92*, 9135–9152.

Clifford, S. M. (1993), A model for the hydrologic and climatic behavior of water on Mars, *J. Geophys. Res.*, *98*, 10,973–11,016.

Craddock, R. A., and R. Greeley (1994), Geologic map of the MTM-20147 Quadrangle, Mangala Vallis region of Mars, *U. S. Geol. Surv. Geol. Invest. Ser. Map*, I-2310.

Dohm, J. M., et al. (2001a), Latent outflow activity for western Tharsis, Mars: Significant flood record exposed, *J. Geophys. Res.*, *106*, 12,301–12,314.

Dohm, J. M., J. C. Ferris, V. R. Baker, R. C. Anderson, T. M. Hare, R. G. Strom, N. G. Barlow, K. L. Tanaka, J. E. Klemaszewski, and D. H. Scott (2001b), Ancient drainage basin of the Tharsis region, Mars: Potential source for outflow channel systems and putative oceans or paleolakes, *J. Geophys. Res.*, *106*, 32,943–32,958.

Ernst, R. E., J. W. Head, E. Parfitt, E. Grosfils, and L. Wilson (1995), Giant radiating dyke swarms on Earth and Venus, *Earth Sci. Rev.*, *39*, 1–58.

French, H. M. (1996), *The Periglacial Environment*, 2nd ed., 341 pp., Pitman, London.

Fuller, E. R., and J. W. Head (2002a), Geological history of the smoothest plains on Mars (Amazonis Planitia) and astrobiological implications, *Lunar Planet. Sci.* [CD-ROM], *XXXIII*, Abstract 1539.

Fuller, E. R., and J. W. Head (2002b), Amazonis Planitia: The role of geologically recent volcanism and sedimentation in the formation of the smoothest plains on Mars, *J. Geophys. Res.*, *107*(E10), 5081, doi:10.1029/2002JE001842.

Ghatan, G. J., J. W. Head, L. Wilson, and H. J. Leask (2004), Mangala Valles, Mars: Investigations of the source of flood water and early stages of flooding, *Lunar Planet. Sci.* [CD-ROM], *XXXV*, Abstract 1147.

Ghatan, G. J., J. W. Head, and L. Wilson (2005), Mangala Valles, Mars: Assessment of early stages of flooding and downstream flood evolution, *Earth Moon Planets*, *96*(1–2), 1–57.

Gulick, V. C. (1998), Magmatic intrusions and a hydrothermal origin for fluvial valleys on Mars, *J. Geophys. Res.*, *103*, 19,365–19,387.

Hanna, J. C., and R. J. Phillips (2003), A new model of the hydrologic properties of the Martian crust and implications for the formation of valley networks and outflow channels, *Lunar Planet. Sci.* [CD-ROM], *XXXIV*, Abstract 2027.

Hanna, J. C., and R. J. Phillips (2005a), Tectonic pressurization of aquifers in the formation of Mangala and Athabasca valles on Mars, *Lunar Planet. Sci.* [CD-ROM], *XXXVI*, Abstract 2261.

Hanna, J. C., and R. J. Phillips (2005b), Hydrological modeling of the Martian crust with application to the pressurization of aquifers, *J. Geophys. Res.*, *110*, E01004, doi:10.1029/2004JE002330.

Head, J. W., and L. Wilson (2001), Mars: Geological setting of magma/H_2O interactions, *Lunar Planet. Sci.* [CD-ROM], *XXXII*, Abstract 1215.

Head, J. W., L. Wilson, and K. L. Mitchell (2003), Generation of recent massive water floods at Cerberus Fossae, Mars by dike emplacement, cryospheric cracking, and confined aquifer groundwater release, *Geophys. Res. Lett.*, *30*(11), 1577, doi:10.1029/2003GL017135.

Head, J. W., D. R. Marchant, and G. J. Ghatan (2004), Glacial deposits on the rim of a Hesperian-Amazonian outflow channel source trough: Mangala Valles, Mars, *Geophys. Res. Lett.*, *31*, L10701, doi:10.1029/2004GL020294.

Hecht, C. E. (1990), *Statistical Thermodynamics and Kinetic Theory*, 484 pp., W. H. Freeman, New York.

Hoffman, N. (2000), White Mars: A new model for Mars' surface and atmosphere based on CO_2, *Icarus*, *146*(2), 326–342.

Kaye, G. W. C., and T. H. Laby (1966), *Tables of Physical and Chemical Constraints*, 249 pp., Longman, New York.

Kieffer, H. H., T. Z. Martin, A. R. Peterfreund, and B. M. Jakosky (1977), Thermal and albedo mapping of Mars during the Viking primary mission, *J. Geophys. Res.*, *82*, 4249–4291.

Komar, P. D. (1979), Comparisons of the hydraulics of water flows in Martian outflow channels with flows of similar scale on Earth, *Icarus*, *37*(1), 156–181.

Komatsu, G., and V. R. Baker (1997), Paleohydrology and flood geomorphology of Ares Vallis, *J. Geophys. Res.*, *102*, 4151–4160.

Leask, H. J. (2005), Volcano-ice interactions and related geomorphology at Mangala Valles and Aromatum Chaos, Mars, M.Ph. thesis, 199 pp., Lancaster Univ., Lancaster, U. K.

Malin, M. C. (1976), Age of Martian channels, *J. Geophys. Res.*, *81*, 4825–4845.

Manga, M. (2004), Martian floods at Cerberus Fossae can be produced by groundwater discharge, *Geophys. Res. Lett.*, *31*, L02702, doi:10.1029/2003GL018958.

Mastin, L. G., and D. D. Pollard (1988), Surface deformation and shallow dike intrusion processes at Inyo Craters, Long Valley, California, *J. Geophys. Res.*, *93*, 13,221–13,235.

McEwen, A. S., L. Keszthelyi, M. Milazzo, D. M. Burr, P. Christensen, J. Rice, and M. Malin (2002), Athabasca Valles region: New insights from THEMIS, *Eos Trans. AGU*, *83*(47), Fall Meet. Suppl., Abstract P11B-09.

Mitchell, K. L., F. Leesch, and L. Wilson (2005), Uncertainties in water discharge rate at the Athabasca Valles palaeochannel system, Mars, *Lunar Planet. Sci.* [CD-ROM], *XXXVI*, Abstract 1930.

Nummedal, D., J. J. Gonsiewski, and J. C. Boothroyd (1976), Geological significance of large channels on Mars, International Colloquium of Planetary Geology, *Geol. Romana*, *15*, 407–418.

Ogawa, Y., Y. Yamagishi, and K. Kurita (2003), Evaluation of melting process of the permafrost on Mars: Its implication for surface features, *J. Geophys. Res.*, *108*(E4), 8046, doi:10.1029/2002JE001886.

Ori, G. G., and C. Mosangini (1998), Complex depositional systems in Hydraotes Chaos, Mars: An example of sedimentary process interactions in the Martian hydrological cycle, *J. Geophys. Res.*, *103*, 22,713–22,723.

Plescia, J. B. (2003), Cerberus Fossae, Elysium Mons: A source for lava and water, *Icarus*, *164*(1), 79–95, doi:10.1016/S0019-1035(03)00139-8.

Robinson, M. S., and K. L. Tanaka (1990), Magnitude of a catastrophic flood event at Kasei Valles, Mars, *Geology*, *18*, 902–905.

Rubin, A. M. (1992), Dike-induced faulting and graben subsidence in volcanic rift zones, *J. Geophys. Res.*, *97*, 1839–1858.

Schultz, R. A., C. H. Okubo, C. L. Goudy, and S. J. Wilkins (2004), Igneous dikes on Mars revealed by Mars orbiter laser altimeter topography, *Geology*, *32*(10), 889–892, doi:10.1130/G20548.1.

Sharp, R. P., and M. C. Malin (1975), Channels on Mars, *Geol. Soc. Am. Bull.*, *86*, 593–609.

Squyres, S. W., S. M. Clifford, R. O. Kuzmin, J. R. Zimbelman, and F. M. Costard (1992), Ice in the Martian regolith, in *Mars*, edited by H. H. Kieffer et al., pp. 523–554, Univ. of Ariz. Press, Tucson.

Tanaka, K. L., and M. G. Chapman (1990), The relation of catastrophic flooding of Mangala Valles, Mars, to faulting of Memnonia Fossae and Tharsis volcanism, *J. Geophys. Res.*, *95*, 14,315–14,323.

Tanaka, K. L., M. P. Golombek, and W. B. Banerdt (1991), Reconciliation of stress and structural histories of the Tharsis region of Mars, *J. Geophys. Res.*, *96*, 15,617–15,633.

U.S. Geological Survey (2003), Topographic and color-coded contour maps of Mars, scale 1:25,000,000, *U.S. Geol. Surv. Geol. Invest. Ser. Map*, I-2782.

Wallace, D., and C. Sagan (1979), Evaporation of ice in planetary atmospheres: Ice-covered rivers on Mars, *Icarus*, *39*(3), 385–400.

Wilson, L., and J. W. Head (2001), Giant dike swarms and related graben systems in the Tharsis province of Mars, *Lunar Planet. Sci.* [CD-ROM], *XXXII*, Abstract 1153.

Wilson, L., and J. W. Head (2002), Tharsis-radial graben systems as the surface manifestation of plume-related dike intrusion complexes: Models and implications, *J. Geophys. Res.*, *107*(E8), 5057, doi:10.1029/2001JE001593.

Wilson, L., and J. W. Head (2004), Evidence for a massive phreatomagmatic eruption in the initial stages of formation of the Mangala Valles outflow channel, Mars, *Geophys. Res. Lett.*, *31*(15), L15701, doi:10.1029/2004GL020322.

Wilson, L., J. W. Head, H. J. Leask, G. J. Ghatan, and K. L. Mitchell (2004a), Factors controlling water volumes and release rates in Martian outflow channels, *Lunar and Planet. Sci.* [CD-ROM], *XXXV*, Abstract 1151.

Wilson, L., G. J. Ghatan, J. W. Head, and K. L. Mitchell (2004b), Mars outflow channels: A reappraisal of the estimation of water flow velocities from water depths, regional slopes and channel floor properties, *J. Geophys. Res.*, *109*, E09003, doi:10.1029/2004JE002281.

Zimbelman, J. R., R. A. Craddock, R. Greeley, and R. O. Kuzmin (1992), Volatile history of Mangala Valles, Mars, *J. Geophys. Res.*, *97*, 18,309–18,317.

————————

H. J. Leask and L. Wilson, Planetary Science Research Group, Environmental Science Department, Institute of Environmental and Natural Sciences, Lancaster University, Lancaster LA1 4YQ, UK. (l.wilson@Lancaster.ac.uk)

K. L. Mitchell, Jet Propulsion Laboratory, Mail Stop 183-601, 4800 Oak Grove Drive, Pasadena, CA 91109-8099, USA.